Available online at www.derpharmachemica.com

Scholars Research Library

Der Pharma Chemica, 2015, 7(10):543-555
(http://derpharmachemica.com/archive.html)

ISSN 0975-413X
CODEN (USA): PCHHAX

A theoretical analysis of the relationships between electronic structure and HIV-1 integrase inhibition and antiviral activity of a series of naphthyridinone derivatives

Javier Valdebenito-Gamboa and Juan S. Gómez-Jeria*

Quantum Pharmacology Unit, Department of Chemistry, Faculty of Sciences, University of Chile. Las Palmeras 3425, Santiago, Chile

---

ABSTRACT

A Density Functional Theory study was carried out to find relationships between the electronic structure and antiviral activity, integrase inhibition and protein binding effects in a series of naphthyridinone derivatives. Statistically significant equations were obtained for antiviral and integrase inhibition, and the corresponding 2D pharmacophores were built. These pharmacophores can be employed to select the atoms for future synthesis of more active compounds. In the case of protein binding effects no statistically significant results were obtained. For this last case it is suggested that the experimental numerical results correspond to different action mechanisms.

Keywords: HIV-1 integrase, QSAR, DFT, Naphthyridinone, antiviral activity.

INTRODUCTION

The human immunodeficiency virus (HIV) is a member of the genus *Lentivirus*, part of the family *Retroviridae*. It is the causative agent of HIV infection and acquired immunodeficiency syndrome (AIDS). The life cycle of HIV contains several critical steps which can be used as targets for chemotherapeutic intrusion. In one of these steps the virus must insert DNA copies of its RNA genome into the host chromosomes. This integration is catalyzed by the viral-encoded integrase enzyme (IN). HIV IN is a 32 kDa protein produced from the C-terminal portion of the Pol gene product. Since HIV-1 IN was recognized as a significant antiretroviral drug target, an impressive number of studies were carried out to find molecules inhibiting this enzyme [1-31]. During year 2007, the U.S. FDA approved the IN inhibitor raltegravir. In 2012 the second IN inhibitor, elvitegravir, was approved. These experimental studies have been complemented with theoretical analyses [19, 32-52]. In earlier works we carried out studies with different molecules for HIV-1 reverse transcriptase inhibition, protection against cytopathic effects, cytostatic effects and HIV-1 replication [53-55]. Recently, a group of naphthyridinone derivatives was synthesized and tested for HIV-1 integrase enzyme inhibition, antiviral activity and protein binding effects [56]. Here we present the results of a Density Functional Theory analysis linking several local atomic reactivity indices of the aforementioned molecules with these biological activities.

MATERIALS AND METHODS

METHODS, MODELS AND CALCULATIONS

The QSAR method

Considering that the method employed here has been explained in a very detailed manner in practically every paper we have published on this subject, we decided to refer the reader to the literature [57-63]. Therefore, we shall discuss below only the resulting equations. The master equation relating any biological activity with electronic structure is the only member of the class of model-based methods. It contains local atomic reactivity indices describing almost all possible molecule-site atom-atom interactions. For the case of *in vitro* ligand-site interactions expressed as equilibrium constants (or affinity constants) or IC_{50} values (that are indirectly related to equilibrium constants by the Cheng-Prusoff equation, for the exact relationship see [64]) this method produced excellent results [55, 59, 65-90]. For the case of an *in vivo* or *in vitro* multistep and/or multimechanistic action mechanism our method requires that all the steps and all the mechanisms inside each step be the same for all the group of molecules under analysis. Very good results were obtained for a variety of molecules and biological activities [53, 54, 72, 91-107]. This approach is called the Klopman-Peradejordi-Gómez method (KPG).

Selection of molecules and biological activity

The molecules were selected from a recent study [56] and are shown in Table 1 and Fig. 1. The experimental biological activities analyzed in this paper are the results of a biochemical enzymatic integrase strand-transfer assay ($^{ST}IC_{50}$), a single-round pseudotyped antiviral assay utilizing a luciferase reporter ($^{pHIV}IC_{50}$) and a protein-adjusted IC_{50} ($^{pHIV}PAIC_{50}$, determined using 40 mg/mL of purified human serum albumin in the pHIV assay). A preliminary analysis of the experimental results shows that no statistically significant relationship exists between any couple of them.

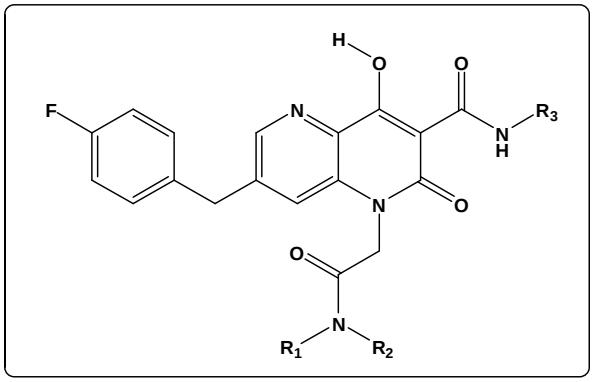

Figure 1. General structure of the selected naphthyridinone derivatives

Calculations

We worked within the common skeleton assumption asserting that there is a set of atoms, common to all the molecules analyzed, that explains almost all the biological activities. The effect of the substituents is to modify the electronic structure of this common skeleton and/or influencing the correct placement of the drug. The common skeleton is presented in Fig. 2, together with the atom numbering used in the resulting statistical equations.

Table 1. Naphthyridinone derivatives and their experimental biological activities

Mol.	R_1	R_2	R_3	Log $^{ST}IC_{50}$	Log $^{pHIV}IC_{50}$	Log $^{pHIV}PAIC_{50}$
1	H	H	Me	0.88	0.34	1.75
2	H	Me	Me	0.97	0.52	1.34
3	Me	Me	Me	0.97	0.77	1.28
4	Et	Et	Me	0.64	0.96	1.23
5	$CH_2CH_2CH_2CH_2$		Me	1.11	0.69	1.20
6	H	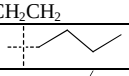	Me	0.96	0.74	1.15
7	H		Me	0.89	0.51	1.08
8	H		Me	0.64	0.41	0.88
9	H	*t*-Bu	Me	0.84	0.68	1.20
10	H	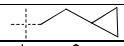	Me	0.90	0.77	1.52
11	H	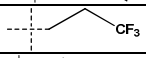	Me	0.85	0.18	1.18
12	H	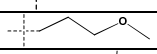	Me	0.83	0.57	1.96
13	H	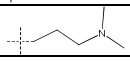	Me	1.34	1.62	1.92
14	H	OMe	Me	0.76	0.52	1.11
15	Me	Me		0.48	0.97	2.29
16	Me	Me	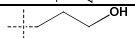	0.76	1.23	1.54
17	Me	Me	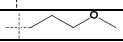	0.60	0.49	0.95
18	Me	Me	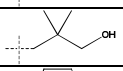	0.81	0.56	1.91
19	Me	Me	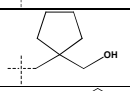	1.36	0.86	1.38
20	Me	Me	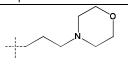	0.93	1.28	1.40
21	H	H	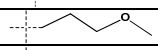	0.89	0.63	1.34
22		H	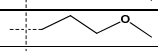	0.86	0.48	1.26
23		H	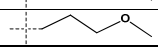	0.93	0.52	1.59
24		H	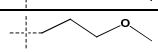	0.79	0.51	1.76
25	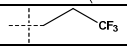	H	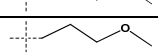	1.04	0.38	1.30
26	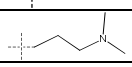	H	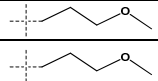	1.65	1.43	2.09
27	$CH_2CH_2CH_2CH_2$		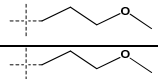	1.62	0.58	1.04
28	$CH_2CH_2CH_2CH_2CH_2$		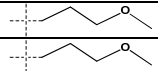	0.67	0.56	1.08
29	$CH_2CH_2OCH_2CH_2$		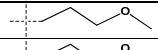	0.88	0.54	0.83
30	$CH_2CH_2N(Me)CH_2CH_2$		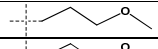	1.45	0.72	1.11

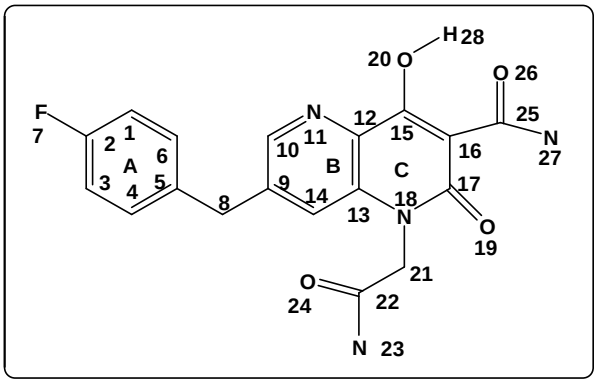

Figure 2. Common skeleton numbering of naphthyridinone derivatives

Molecular geometries were fully optimized at the DFT B3LYP/6-31G(d,p) level of theory with the Gaussian package [108]. From the corrected Mulliken Population Analysis results, we obtained numerical values for all electronic local atomic reactivity indices (LARIS) appearing in the master equation [109, 110]. D-CENT-QSAR software was used for this purpose [111]. Since the system of linear equations cannot be solved because the number of molecules is smaller than the number of unknown coefficients, a linear multiple regression analysis (LMRA) was carried out. The Statistica software was employed [112].

RESULTS

^{pHIV}IC50 Results (antiviral activity).

After successive LMRAs to eliminate the outliers from the original set (n=30), we obtained the following equation:

$$\log(^{pHIV}IC_{50}) = 9.16 + 1.43\mu_{15} - 0.002S_{10}^{N}(LUMO+2)^{*} - 2.66S_{9}^{E}(HOMO-2)^{*} + \\ +3.67S_{18}^{N}(LUMO)^{*} - 3.69s_{8} - 1.20S_{25}^{N}(LUMO+1)^{*} \quad (1)$$

with n=28, R=0.96, R^2=0.92, adj R^2=0.90, F(6,21)=42.95 (p<0.000001) and SD=0.09. No outliers were detected and no residuals fall outside the ±2σ limits. Here, μ_{15} is the local atomic electronic chemical potential of atom 15, $S_{10}^{N}(LUMO+2)^{*}$ is the nucleophilic superdelocalizability of the third lowest vacant MO localized on atom 10, $S_{9}^{E}(HOMO-2)^{*}$ is the electrophilic superdelocalizability of the third highest occupied MO localized on atom 9, $S_{18}^{N}(LUMO)^{*}$ is the nucleophilic superdelocalizability of the lowest vacant MO localized on atom 18, s_8 is the local atomic softness of atom 8 and $S_{25}^{N}(LUMO+1)^{*}$ is the nucleophilic superdelocalizability of the second lowest MO localized on atom 25. Table 2 displays the beta coefficients and the results of the t-test for significance of coefficients of Eq. 1. Table 3 shows the squared correlation coefficients for the independent variables appearing in Eq. 1, showing that there are no significant internal correlations. Fig. 3 shows the plot of observed *vs.* calculated log(^{pHIV}IC50) values. The associated statistical parameters of Eq. 1 indicate that this equation is statistically significant and that the variation of the numerical value of a group of six local atomic reactivity indices of atoms of the common skeleton explains about 90% of the variation of the antiviral activity.

Table 2. Beta coefficients and *t*-test for significance of the coefficients in Eq. 1

Variable	Beta	t(21)	p-level
μ_{15}	0.92	12.62	<0.000001
$S_{10}^{N}(LUMO+2)^{*}$	-0.51	-8.13	<0.000001
$S_{9}^{E}(HOMO-2)^{*}$	-0.78	-9.70	<0.000001
$S_{18}^{N}(LUMO)^{*}$	0.65	6.97	<0.000001
s_8	-0.28	-3.98	<0.0007
$S_{25}^{N}(LUMO+1)^{*}$	-0.18	-2.81	<0.01

$^{pHIV}PAIC_{50}$ Results (protein binding effects).

No statistically significant equation was obtained for the whole set. We created a new set without including the five highest experimental values. No statistically significant equation was obtained. Another set built without the lowest five experimental values did not produce any statistically significant result. For all the LRMA results no outliers were detected and no residuals fall outside the ±2σ limits. The only possible explanation is that the action mechanism(s) producing the $^{pHIV}PAIC_{50}$ experimental values is not the same for all the molecules. We have commented on this possibility earlier as possible source of failure of the method employed here [53].

Table 3. Matrix of squared correlation coefficients for the variables appearing in Eq. 1

	μ_{15}	$S_{10}^{N}(LUMO+2)*$	$S_{9}^{E}(HOMO-2)*$	$S_{18}^{N}(LUMO)*$	S_8
μ_{15}	1				
$S_{10}^{N}(LUMO+2)*$	0.0001	1			
$S_{9}^{E}(HOMO-2)*$	0.008	0.02	1		
$S_{18}^{N}(LUMO)*$	0.1	0.02	0.3	1	
S_8	0.002	0.006	0.0009	0.1	1
$S_{25}^{N}(LUMO+1)*$	0.05	0.04	0.0004	0.01	0.0001

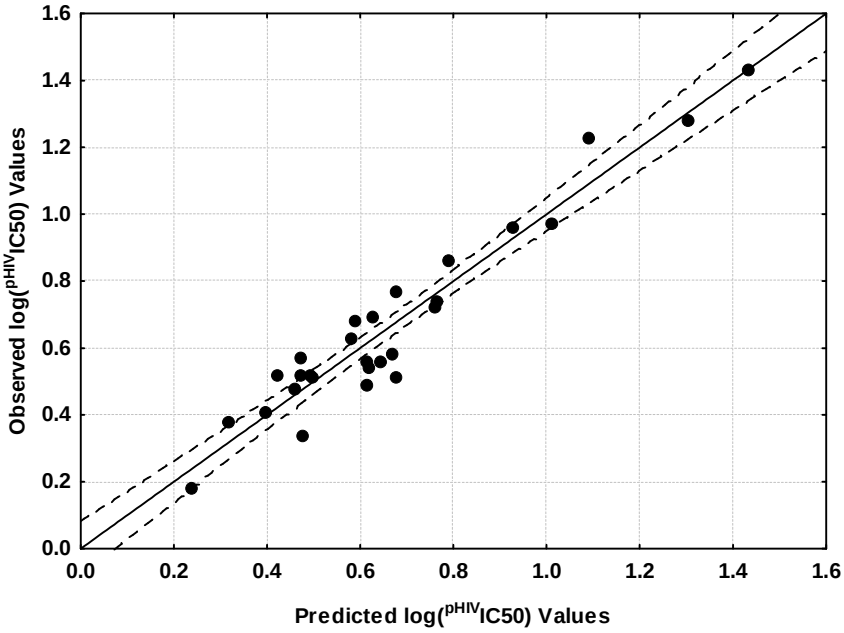

Figure 3. Plot of predicted *vs.* observed log(^{pHIV}IC50) values from Eq. 1. Dashed lines denote the 95% confidence interval

STIC50 Results (inhibition of the strand transfer step of HIV-1 integrase).

After successive LMRAs to eliminate the outliers from the original set (n=30), we obtained the following equation:

$$\log(^{ST}IC_{50}) = 1.78 - 0.57S_{24}^{E}(HOMO-1)* - 0.002S_{10}^{N}(LUMO+2)* + 0.24S_{15}^{N}(LUMO)* + 0.006S_{14}^{N}(LUMO+2)* + 0.28S_{7}^{N}(LUMO+2)* + 0.0008S_{23}^{N}(LUMO+1)* \quad (2)$$

with n=27, R=0.97, R^2=0.94, adj R^2=0.92, F(6,20)=56.64 (p<0.000001) and SD=0.08. No outliers were detected and no residuals fall outside the ±2σ limits. Here, $S_{24}^{E}(HOMO-1)*$ is the electrophilic superdelocalizability of the second highest occupied MO localized on atom 24, $S_{10}^{N}(LUMO+2)*$ is the nucleophilic superdelocalizability of the third lowest MO localized on atom 10, $S_{15}^{N}(LUMO)*$ is the nucleophilic superdelocalizability of the lowest vacant MO localized on atom 15, $S_{14}^{N}(LUMO+2)*$ is the nucleophilic superdelocalizability of the third lowest vacant MO localized on atom 14, $S_{7}^{N}(LUMO+2)*$ is the nucleophilic superdelocalizability of the third lowest MO localized on atom 7 and $S_{23}^{N}(LUMO+1)*$ is the nucleophilic superdelocalizability of the second lowest MO

localized on atom 23. Table 4 displays the beta coefficients and the results of the t-test for significance of coefficients of Eq. 2. Table 5 shows the squared correlation coefficients for the independent variables appearing in Eq. 2, showing that there are no significant internal correlations. Fig. 4 displays the plot of observed *vs.* calculated log(STIC50) values. The associated statistical parameters of Eq. 2 indicate that this equation is statistically significant and that the variation of the numerical value of a group of six local atomic reactivity indices belonging to atoms of the common skeleton explains about 92% of the variation of the inhibition of the strand transfer step of HIV-1 integrase.

Table 4. Beta coefficients and *t*-test for significance of the coefficients in Eq. 2

Variable	Beta	t(20)	p-level
$S_{24}^{E}(HOMO-1)*$	-0.55	-9.66	0.000000
$S_{10}^{N}(LUMO+2)*$	-0.58	-10.00	<0.000001
$S_{15}^{N}(LUMO)*$	0.42	6.82	<0.000001
$S_{14}^{N}(LUMO+2)*$	0.52	9.15	<0.000001
$S_{7}^{N}(LUMO+2)*$	0.22	3.86	<0.001
$S_{23}^{N}(LUMO+1)*$	0.20	3.39	<0.003

Table 5. Matrix of squared correlation coefficients for the variables appearing in Eq. 2

	$S_{24}^{E}(HOMO-1)*$	$S_{10}^{N}(LUMO+2)*$	$S_{15}^{N}(LUMO)*$	$S_{14}^{N}(LUMO+2)*$	$S_{7}^{N}(LUMO+2)*$
$S_{10}^{N}(LUMO+2)*$	0.02	1			
$S_{15}^{N}(LUMO)*$	0.08	0.0001	1		
$S_{14}^{N}(LUMO+2)*$	0.0004	0.0004	0.07	1	
$S_{7}^{N}(LUMO+2)*$	0.01	0.0009	0.08	0.003	1
$S_{23}^{N}(LUMO+1)*$	0.003	0.1	0.03	0.01	0.005

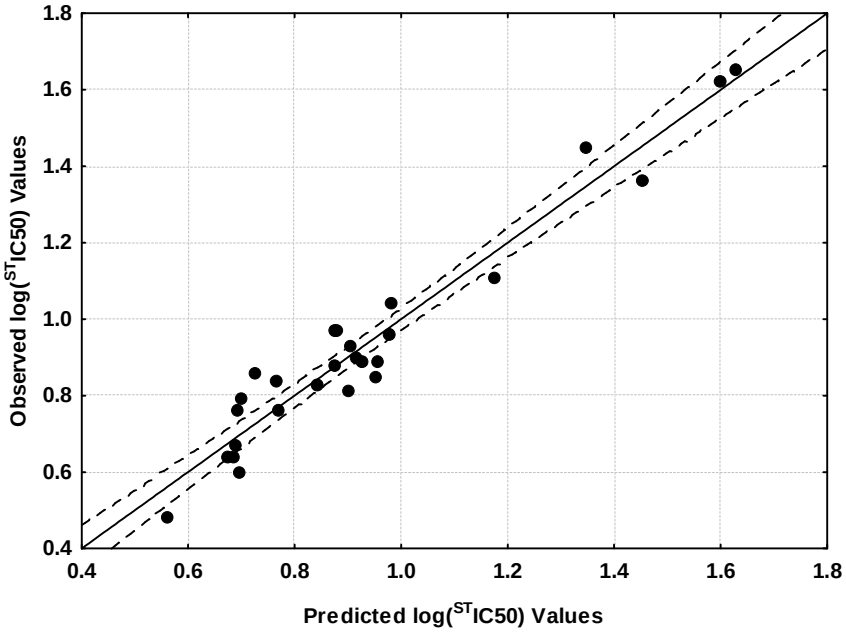

Figure 4. Plot of predicted *vs.* observed log(STIC50) values from Eq. 2. Dashed lines denote the 95% confidence interval

Table 6. Local molecular orbitals of atoms 7, 9 and 10

Mol.	Atom 7 (F)	Atom 9 (C)	Atom 10 (C)
1 (100)	98π99π100π-104π108π111π	98π99π100π-101π102π104π	97π99π100π-101π102π105π
2 (104)	92π102π103π-108π112π115π	102π103π104π-105π106π108π	98σ100π104π-105π106π109π
3 (108)	102π105π106π-111π112π117π	106π107π108π-109π110π111π	105σ107π108π-109π110π111π
4 (116)	103π109π113π-120π125141π	113σ115π116π-117π118π119π	114π115π116π-117π118π119π
5 (115)	113π114π115π-119π121π124π	113π114σ115π-116π117π119π	109σ114π115π-116π117π120π
6 (112)	110π111π112π-116π117π120π	110π111σ112π-113π114π116π	110π111π112π-113π114π117π
7 (112)	110π111π112π-116π117π120π	110π111π112π-113π114π115π	106σ111π112π-113π114π117π
8 (111)	97π110π111π-115π116π120π	109π110π111π-112π113π115π	109π110π111π-112π113π114π
9 (116)	102π114π115π-120π125π127π	114σ115π116π-117π118π120π	112π115π116π-117π118π121π
10 (115)	101π114π115π-119π120π124π	113π114π115π-116π117π119π	113π114π115π-116π117π118π
11 (120)	115π119π120π-125π126π128π	118π119π120π-121π122π123π	118π119π120π-121π122π124π
12 (116)	114π115π116π-120π121π124π	114π115π116π-117π118π120π	109σ115π116π-117π118π121π
13 (120)	117π118π119π-124π125π128π	117π118π119π-121π122π124π	113σ118π119π-121π122π125π
14 (108)	106π107π108π-113π114π116π	106π107π108π-109π110π112π	104π107π108π-109π110π112π
15 (115)	100π101π114π-119π124π127π	113π114σ115π-116π117π119π	113π114σ115π-116π117π119π
16 (116)	102π109π113π-120π125π129π	113σ115π116π-117π118π119π	113σ115π116π-117π118π119π
17 (120)	112π113π116π-124π129π133π	118π119π120π-121π122π123π	116σ119π120π-121π122π123π
18 (124)	109π117π121π-127π128π133π	122π123π124π-125π126π127π	121σ123π124π-125π126π127π
19 (131)	113π128π129π-135π136π140π	125π129σ131π-132π133π134π	128π129π131π-132π133π134π
20 (135)	119π126π130π-138π139π144π	130σ133π135π-136π137π138π	130σ133π135π-136π137π138π
21 (112)	98π110π111π-116π120π124π	110π111π112π-113π114π116π	106σ108π112π-113π114π117π
22 (123)	107π122π123π-127π128π132π	121π122π123π-124π125π127π	121π122π123π-124π125π126π
23 (127)	111π126π127π-132π136π140π	125π126π127π-128π129π131π	125π126π127π-128π129π130π
24 (124)	122π123π124π-128π129π132π	122π123π124π-125π126π128π	118π123π124π-125π126π129π
25 (132)	118π131π132π-137π138π140π	130π131π132π-133π134π135π	130π131π132π-133π134π136π
26 (132)	129π130π131π-136π137π140π	129π130π131π-133π134π136π	124σ130π131π-133π134π137π
27 (127)	125π126π127π-131π133π136π	125π126σ127π-128π129π131π	121σ126π127π-128π129π132π
28 (131)	115π130π131π-135π136π139π	129π130π131π-132π133π135π	128π130π131π-132π133π134π
29 (131)	129π130π131π-136π139π147π	129π130π131π-132π133π135π	129π130π131π-132π133π134π
30 (135)	118π129π130π-139π143π144π	130σ133π134π-136π137π138π	129π130π134π-136π137π138π

Table 7. Local molecular orbitals of atoms 14, 15 and 18

Mol.	Atom 14 (C)	Atom 15 (C)	Atom 18 (N)
1 (100)	95σ99π100π-101π102π103π	95σ98π99-101π103π105π	98π99π100π-101π102π105π
2 (104)	98σ103π104π-105π106π107π	98σ102π103-105π107π109π	102π103π104π-105π106π109π
3 (108)	105π107π108π-109π110π111π	104π107π108-109π113π115π	104π107π108π-109π110π111π
4 (116)	113σ115π116π-117π118π119π	112π115π116-117π121π123π	114π115π116π-117π118π119π
5 (115)	113π114π115π-116π117π119π	109σ113π114π-116π119π121π	113π114π115π-116π117π119π
6 (112)	105π110π111π-113π114π116π	106σ110π111π-113π115π116π	110π111π112π-113π114π116π
7 (112)	105σ110π111π-113π114π116π	106σ110π111π-113π115π116π	110π111π112π-113π114π116π
8 (111)	106π109π110π-112π113π115π	105σ106π109π-112π114π115π	109π110π111π-112π113π115π
9 (116)	110σ115π116π-117π118π119π	114π115π116π-117π119π121π	112π114π116π-117π118π121π
10 (115)	111σ113π114π-116π117π119π	109σ110π113π-116π118π119π	113π114π115π-116π117π119π
11 (120)	116π118π119π-121π122π124π	115σ116π118π-121π1π23π124π	118π119π120π-121π122π123π
12 (116)	107π114π115π-117π118π120π	109σ114π115π-117π11π9π120π	114π115π116π-117π118π119π
13 (120)	112π117π118π-121π122π124π	113σ117π118π-121π123π124π	117π118π119π-121π122π123π
14 (108)	103π106π107π-109π110π112π	102σ103π106π-109π111π112π	106π107π108π-109π110π111π
15 (115)	113π114π115π-116π117π121π	111σ113π115π-116π119π1π20π	113π114π115π-116π117π120π
16 (116)	113σ115π116π-117π118π119π	112π115π116π-117π121π123π	112π115π116π-117π118π121π
17 (120)	116σ119π120π-121π122π123π	115π119π120π-121π125π127π	114π119π120π-121π122π125π
18 (124)	121π123π124π-125π126π127π	120σ123π124π-125π129π131π	119π123π124π-125π126π127π
19 (131)	125π126π128π-132π133π135π	128π129π131π-132π133π134π	128π129π131π-132π133π135π
20 (135)	127σ133π135π-136π137π138π	130σ133π135π-136π140π142π	133π134π135π-136π137π138π
21 (112)	110π111π112π-113π114π115π	106σ110π111π-113π115π117π	110π111π112π-113π114π117π
22 (123)	117π121π122π-124π125π127π	115σ116σ121π-124π126π127π	121π122π123π-124π125π127π
23 (127)	121π125π126π-128π129π131π	119π120π125π-128π130π131π	125π126π127π-128π129π130π
24 (124)	116π122π123π-125π126π128π	117σ122π123π-125π127π128π	122π123π124π-125π126π127π
25 (132)	127π130π131π-133π134π136π	126σ127π130π-133π135π136π	130π131π132π-133π134π135π
26 (132)	123π129π130π-133π134π136π	124σ129π130π-133π135π136π	129π130π131π-133π134π135π
27 (127)	125π126π127π-128π129π131π	119σ120σ125π-128π131π132π	125π126π127π-128π129π131π
28 (131)	128π129π130π-132π133π135π	124σ128π129π-132π134π135π	129π130π131π-132π133π135π
29 (131)	125π128π130π-132π133π135π	124σ128π129π-132π134π135π	128π130π131π-132π133π134π
30 (135)	129π133π134π-136π137π138π	129π130π133π-136π140π141π	132π133π134π-136π137π140π

Local Molecular Orbitals

Tables 6-8 show the local molecular orbital structure of several atoms appearing in Eqs. 1 and 2 (nomenclature: molecule (HOMO) / (HOMO-2)* (HOMO-1)* (HOMO)*-(LUMO)* (LUMO+1)* (LUMO+2)*).

Table 8. Local molecular orbitals of atoms 23, 24 and 25

Mol.	Atom 23 (N)	Atom 24 (O)	Atom 25 (C)
1 (100)	94π97σ99σ-105π106π123π	98π99π100π-105π106π122π	86π93π97π-101π102π104π
2 (104)	101π102π104π-109π110π117π	102π103π104π-109π110π117π	90π96σ100π-105π106π108π
3 (108)	105π106π107π-113π114π115π	106π107π108π-113π114π115π	102σ103σ104π-109π110π111π
4 (116)	114π115π116-121π122π123π	114π115π116π-121π122π123π	109σ110σ112π-117π118π119π
5 (115)	110σ112π114σ-120π121π126π	113π114π115π-119π12π0121π	99π108σ110π-116π117π120π
6 (112)	109π110π111π-116π117π118π	110π111π112π-116π117π118π	104σ105σ107π-113π114π115π
7 (112)	109π110π111σ-116π117π118π	110π111π112π-116π117π118π	104σ105σ107π-113π114π115π
8 (111)	106σ108π109σ-115π116π117π	109π110π111π-115π116π117π	103σ104σ106π-112π113π116π
9 (116)	112π113π116π-121π122π129π	114π115π116π-121π122π144π	99π108σ112π-117π118π120π
10 (115)	110π111π113π-119π120π121π	113π114π115π-119π120π121π	108σ110π111π-116π117π118π
11 (120)	116π118π119π-124π125π126π	116π118π119π-123π124π125π	106π114σ116π-121π122π123π
12 (116)	113π114π115π-120π121π122π	114π115π116π-120π121π122π	107σ108σ111π-117π118π119π
13 (120)	115π117π118π-124π125π126π	117π118π119π-124π125π126π	111σ112σ115π-121π122π123π
14 (108)	104π106σ107σ-112π113π114π	104π106π107π-112π113π114π	93π101σ103π-109π110π111π
15 (115)	113π114π115π-120π121π122π	113π114π115π-120π121π122π	106σ109σ112σ-116π117π119π
16 (116)	113π114π115π-121π122π123π	114π115π116π-121π122π123π	108σ110σ112π-117π118π119π
17 (120)	117π118π119π-125π126π127π	118π119π120π-125π126π127π	112σ113σ115π-121π122π123π
18 (124)	121π122π123π-129π130π131π	122π123π124π-129π130π131π	116σ119π120σ-125π126π127π
19 (131)	126π127π128π-135π136π137π	127π128π129π-135π136π137π	128σ130σ131π-132π138π139π
20 (135)	132π133π135π-140π141π142π	132π133π135π-140π141π142π	129σ131π133σ-136π137π138π
21 (112)	108σ110σ112π-117π118π136π	110π111π112π-117π118π136π	96π104σ108π-113π114π116π
22 (123)	119π120π121σ-127π128π129π	121π122π123π-127π128π129π	114σ115σ117π-124π125π128π
23 (127)	122π123π125π-131π132π133π	125π126π127π-130π131π132π	118σ119σ121π-128π129π130π
24 (124)	120π122σ123σ-128π129π130π	122π123π124π-128π129π130π	106σ115σ118π-125π126π127π
25 (132)	127π130σ131σ-136π137π138π	127π130π131π-135π136π137π	116π125σ127π-133π134π135π
26 (132)	129π130σ132π-136π137π138π	129π130π131π-136π137π138π	122σ123σ125π-133π134π135π
27 (127)	124π125σ126σ-131π132π133π	125π126π127π-131π132π133π	118σ119σ121π-128π129π132π
28 (131)	128π129π130π-135π136π137π	129π130π131π-135π136π137π	122σ123π125π-132π133π134π
29 (131)	129π130π131π-135π136π137π	129π130π131π-134π135π136π	122σ123σ125π-132π133π134π
30 (135)	133π134σ135π-141π142π143π	133π134π135π-140π141π142π	119σ127σ128π-136π137π138π

DISCUSSION

Discussion of ^{pHIV}IC50 Results (antiviral activity)

The beta values (Table 2) indicate that the importance of the variables is $\mu_{15} > S_9^E(HOMO-2)* > S_{18}^N(LUMO)* > S_{10}^N(LUMO+2)* >> s_8 > S_{25}^N(LUMO+1)*$. A high antiviral activity is then associated with high negative values of μ_{15} and s_8, and with low negative numerical values for $S_9^E(HOMO-2)*$. The case of the nucleophilic superdelocalizabilities will be analyzed case by case below. Atom 15 is a carbon in ring C. A higher activity is associated with higher negative values of the local atomic chemical potential. μ_{15} is the midpoint between $HOMO_{15}^*$ and $LUMO_{15}^*$ energies. Both MOs are of π nature (Table 7). $LUMO_{15}^*$ and $HOMO_{15}^*$ do not always coincide with the molecular LUMO and HOMO (Table 7). Considering that a higher negative value of μ_{15} can be obtained by suppressing $HOMO_{15}^*$ and/or by lowering the energy of $LUMO_{15}^*$ we suggest that atom 15 is interacting with an electron-rich center. Atom 10 is a carbon in ring B. $HOMO_{10}^*$, $LUMO_{10}^*$, $(LUMO+1)_{10}^*$ and $(LUMO+2)_{10}^*$ are of π nature (Table 6). Local $(LUMO+2)_{10}$ appears in eq. 1. If $S_{10}^N(LUMO+2)*$ is positive, then a higher activity is associated with higher values of this index. Higher values for this index are obtained by lowering the $(LUMO+2)_{10}$ energy. This, in turn, will push downwards the energies of the first two vacant local MOs, making them more reactive. If negative, low values of $\left|S_{10}^N(LUMO+2)*\right|$ are necessary for high activity. These values are obtained also by lowering the $(LUMO+2)_{10}^*$ energy. Therefore, we suggest that atom 10 is interacting with an electron-rich center through its first three vacant local MOs. Atom 9 is a carbon in ring B. $HOMO_9$ has a π nature (Table 6). With some exceptions, $(HOMO-1)_9^*$ and $(HOMO-2)_9^*$ have also a π nature. A high activity is associated with low negative values for $S_9^E(HOMO-2)*$. This is obtained by shifting downwards the associated eigenvalue, making this local MO less reactive. The appearance of $(HOMO-2)_9^*$ indicates that the first two highest occupied local MOs also participate in the interaction. Joining these three facts, we suggest that atom 9 is interacting with an electron-deficient center but with a repulsive interaction of $(HOMO-2)_9^*$ with an occupied MO of the site. Atom 18 is nitrogen in ring C. Table 7 shows that the three highest occupied local MOs and the three

lowest local vacant ones have a π nature. If the values of $S_{18}^{N}(LUMO)*$ are positive, then a high activity is associated with small positive values of this index. If the values of $S_{18}^{N}(LUMO)*$ are negative, then a high activity is associated with high negative values for this index. In both cases, the desired effect is obtained by shifting upwards the energy of the $(LUMO)_{18}^{*}$ eigenvalue. For these reasons we suggest that atom 18 is acting as an electron donor and it is probably interacting with an electron deficient center. Atom 8 is the carbon of the CH_2 group linking rings A and B. All MOs are of σ nature. S_8, the local atomic softness of atom 8, is always a positive number. Therefore, a high activity is associated with high numerical values for this index. Being this index the inverse of the local atomic hardness of atom 8, high values will be obtained by diminishing the $HOMO_8^{*}$-$LUMO_8^{*}$ distance.

Table 9: Local Molecular Orbitals of atom 8

Mol.	Atom 8		Mol.	Atom 8
1 (100)	95 98 99-**101**104107		16 (116)	105109113-118120123
2 (104)	98102103-**105**108111		17 (120)	109113116-122124127
3 (108)	101102105-110112115		18 (124)	113117121-126128131
4 (116)	106109113-118120123		19 (131)	120121129-133134136
5 (115)	105109114-118119122		20 (135)	123126130-**136**137139
6 (112)	102106**112**-115117119		21 (112)	102106111-**113**116119
7 (112)	102106**112**-115117119		22 (123)	112116122-128130132
8 (111)	101105110-116118120		23 (127)	120126**127**-132134136
9 (116)	110114115-**117**120123		24 (124)	113117**124**-127129131
10 (115)	109114**115**-118120122		25 (132)	122126**132**-135137139
11 (120)	111115**120**-123125127		26 (132)	120124131-135137139
12 (116)	106109**116**-119121123		27 (127)	116120126-130131134
13 (120)	109113119-123125127		28 (131)	124130**131**-136138139
14 (108)	99102**108**-111114115		29 (131)	119124**131**-136138139
15 (115)	105108114-117118119		30 (135)	123126130-**136**139141

We can see that in some molecules the local HOMO (a σ MO) coincides with the molecule's HOMO (6, 7, 10-12, 14, 23-25, 28 and 29) while in other the local LUMO (a σ MO) coincides with the molecule's LUMO (1, 2, 9, 20, 21, and 30). For the first case we may diminish the $HOMO_8$-$LUMO_8$ distance by a proper substitution localizing the molecular LUMO on atom 8, while for the last case we need to localize the molecular HOMO on atom 8. There are some molecules in which neither the local HOMO nor the local LUMO match the molecular frontier orbitals. Therefore, and from the information obtained in this study, we are not in position to suggest a specific $atom_8$-site interaction. But we may confidently state that this interaction involves σ electrons from both partners. Atom 25 is a carbon bonded to carbonyl oxygen and to a nitrogen atom. $S_{25}^{N}(LUMO+1)*$ is involved in the regulation of the biological activity. $LUMO_{25}^{*}$ and $(LUMO+1)_{25}^{*}$ are of π nature in all molecules. Moreover, $LUMO_{25}^{*}$ corresponds to the molecules' LUMO. Following an analogous reasoning used for atom 10, we suggest that atom 25 is interacting with an electron-rich center through its first two vacant local MOs. This is a logical conclusion considering that atom 25 is attached to two more electronegative atoms, O and N. All the above suggestions are shown in the partial 2D pharmacophore of Fig. 5.

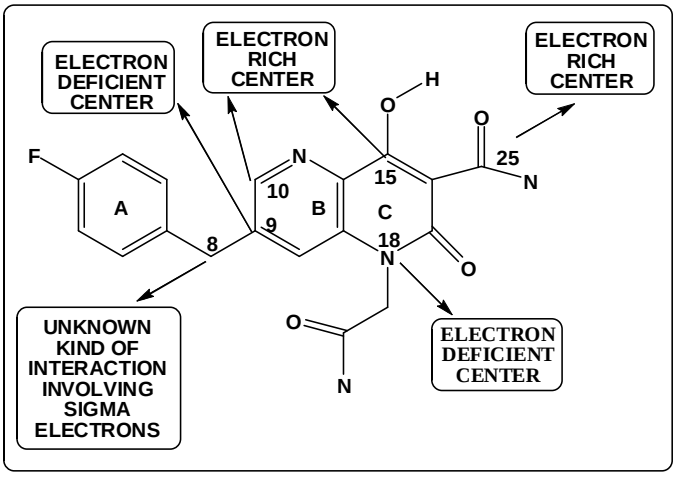

Figure 5. Partial 2D pharmacophore for antiviral activity

Discussion of STIC50 Results (inhibition of the strand transfer step of HIV-1 integrase).

The beta values (Table 4) indicate that the importance of the variables is $S_{10}^{N}(LUMO+2)^*$ > $S_{24}^{E}(HOMO-1)^*$ > $S_{14}^{N}(LUMO+2)^*$ > $S_{15}^{N}(LUMO)^*$ >> $S_{7}^{N}(LUMO+2)^*$ > $S_{23}^{N}(LUMO+1)^*$. A high antiviral activity is then associated with low negative values for $S_{24}^{E}(HOMO-1)^*$. The case of the nucleophilic superdelocalizabilities will be analyzed case by case below. Atom 10 is a carbon of ring B (Fig. 2). The three lowest empty MOs are of π nature (Table 6). If the numerical values of $S_{10}^{N}(LUMO+2)^*$ are positive, a high activity is associated with high numerical values for this index. If negative, high activity is associated with low negative values. Both cases demand that the $(LUMO+2)_{10}^{*}$ eigenvalue be shifted downwards in the energy axis. Therefore, we suggest that atom 10 is interacting, through its three lowest vacant local MOs, with an electron rich center. Atom 24 is the oxygen of the $CH_2C(N)O$ moiety attached to N18 of ring C (Fig. 2). The three highest occupied local MOs are of π nature (Table 8). A high activity is associated with low negative values of $S_{24}^{E}(HOMO-1)^*$. This suggests that this MO could be engaged in a repulsive interaction with occupied MOs of the partner and that the optimum situation should correspond to the interaction of the $HOMO_{24}^{*}$ with one or more empty MOs of the site. Atom 14 is a carbon of ring B (Fig. 2). The first three lowest vacant local MOs are of π nature (Table 7). If the numerical values of $S_{14}^{N}(LUMO+2)^*$ are positive, a high activity is associated with low positive numerical values. These values are obtained by shifting upwards the corresponding eigenvalue in the energy axis, making this MO less prone to interact with occupied MOs of the site. The same situation occurs if the numerical values of $S_{14}^{N}(LUMO+2)^*$ are negative. Therefore, it is suggested that atom 14 interacts with an electron rich center through its first two lowest vacant local MOs. Atom 15 is a carbon of ring C (Fig. 2). $LUMO_{15}^{*}$ has a π nature in all molecules (Table 7). If $S_{15}^{N}(LUMO)^*$ is positive, low numerical values of this index are associated with high activity. These values are obtained by shifting upwards the energy of the corresponding eigenvalue. Therefore, we suggest that atom 15 is interacting with an electron deficient center. Atom 7 is the fluorine atom bonded to atom C2 (Fig. 2). The first three lowest vacant MOs have π nature (Table 6). If the numerical values of $S_{7}^{N}(LUMO+2)^*$ are positive, low values are associated with high activity. These values are obtained by shifting upwards the energy of the corresponding eigenvalue, making $(LUMO+2)_{7}^{*}$ less reactive. A similar situation occurs if the numerical values of $S_{7}^{N}(LUMO+2)^*$ are negative. Therefore, it is suggested that atom 7 is interacting with an electron rich center through its first two lowest vacant MOs (halogen bond?). Atom 23 is the nitrogen of the $CH_2C(N)O$ moiety attached to N18 of ring C (Fig. 2). The first three lowest local vacant MOs are of π nature (Table 8). If the values of $S_{23}^{N}(LUMO+1)^*$ are positive, a low value of this index is associated with high activity. These values are obtained by shifting upwards the energy of the corresponding eigenvalue. Therefore, it is suggested that atom 23 is interacting with an electron rich center through its $LUMO_{23}^{*}$. All these suggestions are included in the 2D pharmacophore shown in Fig. 6.

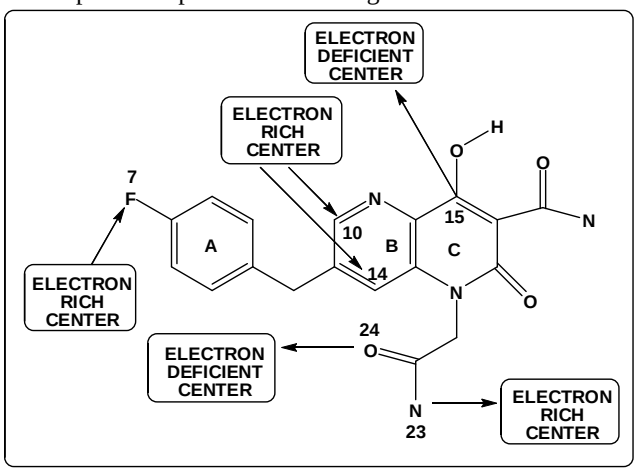

Figure 6. Partial 2D pharmacophore for

From the historical point of view, the size of the molecules employed for QSAR studies has grown as a result of the increasing computational power. In the earlier days of Quantum Pharmacology, SCF *ab initio*, PPP, EHT, CNDO/2, PCILO, INDO, etc. methods were employed for conformational and electronic structure calculations for relatively small molecules [113-117]. In these cases the pharmacophores were easily suggested. Today the molecules that are studied have several dozens of atoms and, with some exceptions, have a great conformational flexibility. For this reason we always present our pharmacophores as two-dimensional drawings. With the method used here, the pharmacological active conformation is not easy to detect. It is worth to mention that the interpretation of the local reactivity indices appearing in Eq. 1 and 2 is in agreement with "intuitive" organic chemistry: an electron rich atom interacts with an electron deficient center and so on.

CONCLUSION

Satisfactory statistically significant equations were obtained for the antiviral activity and HIV-1 integrase inhibition for a series of naphthyridinone derivatives. From the pharmacophores built from our results it is possible to select one or more atoms for substitution to synthesize compounds with enhanced activity.

REFERENCES

[1] Y Wang, J Rong, B Zhang, L Hu, X Wang, et al., *Bioorg. Med. Chem.*, **2015**, 23, 735-741.
[2] H Wang, MD Kowalski, AS Lakdawala, FG Vogt, L Wu, *Org. Lett.*, **2015**, 17, 564-567.
[3]V Tandon, Urvashi, P Yadav, S Sur, S Abbat, et al., *ACS Med. Chem. Lett.*, **2015**, 10. 1021 /acsmedchemlett.5b00230,
[4] RV Patel, SW Park, *Bioorg. Med. Chem.*, **2015**, 23, 5247-5263.
[5] RV Patel, Y-S Keum, SW Park, *Eur. J. Med. Chem.*, **2015**, 97, 649-663.
[6] BN Naidu, ME Sorenson, M Patel, Y Ueda, J Banville, et al., *Biorg. Med. Chem. Lett.*, **2015**, 25, 717-720.
[7] G Cuzzucoli-Crucitti, L Pescatori, A Messore, VN Madia, G Pupo, et al., *Eur. J. Med. Chem.*, **2015**, 101, 288-294.
[8] XZ Zhao, SJ Smith, M Métifiot, BC Johnson, C Marchand, et al., *J. Med. Chem.*, **2014**, 57, 1573-1582.
[9] D Zhang, B Debnath, S Yu, TW Sanchez, F Christ, et al., *Bioorg. Med. Chem.*, **2014**, 22, 5446-5453.
[10] V Suchaud, F Bailly, C Lion, C Calmels, M-L Andréola, et al., *J. Med. Chem.*, **2014**, 57, 4640-4660.
[11] KK Reddy, SK Singh, *Chem-Biol. Int.*, **2014**, 218, 71-81.
[12] TO Olomola, S Mosebi, R Klein, T Traut-Johnstone, J Coates, et al., *Bioorg. Chem.*, **2014**, 57, 1-4.
[13] TO Olomola, R Klein, PT Kaye, *Tetrahedron*, **2014**, 70, 9449-9455.
[14] B-W Li, F-H Zhang, E Serrao, H Chen, TW Sanchez, et al., *Bioorg. Med. Chem.*, **2014**, 22, 3146-3158.
[15] W-G Gu, X Zhang, D Tsz-Ming, L-M Yang, Y-T Zheng, et al., *FEBS Lett.*, **2014**, 588, 3461-3468.
[16] W-g Gu, DT-M Ip, S-j Liu, JH Chan, Y Wang, et al., *Chem-Biol. Int.*, **2014**, 213, 21-27.
[17] LD Fader, E Malenfant, M Parisien, R Carson, F Bilodeau, et al., *ACS Med. Chem. Lett.*, **2014**, 5, 422-427.
[18] S Yu, TW Sanchez, Y Liu, Y Yin, N Neamati, et al., *Biorg. Med. Chem. Lett.*, **2013**, 23, 6134-6137.
[19] H Sharma, TW Sanchez, N Neamati, M Detorio, RF Schinazi, et al., *Biorg. Med. Chem. Lett.*, **2013**, 23, 6146-6151.
[20] E Serrao, Z-L Xu, B Debnath, F Christ, Z Debyser, et al., *Bioorg. Med. Chem.*, **2013**, 21, 5963-5972.
[21] T Kawasuji, BA Johns, H Yoshida, JG Weatherhead, T Akiyama, et al., *J. Med. Chem.*, **2013**, 56, 1124-1135.
[22] BA Johns, T Kawasuji, JG Weatherhead, T Taishi, DP Temelkoff, et al., *J. Med. Chem.*, **2013**, 56, 5901-5916.
[23] BA Johns, T Kawasuji, JG Weatherhead, EE Boros, JB Thompson, et al., *Biorg. Med. Chem. Lett.*, **2013**, 23, 422-425.
[24] M Billamboz, V Suchaud, F Bailly, C Lion, J Demeulemeester, et al., *ACS Med. Chem. Lett.*, **2013**, 4, 606-611.
[25] XZ Zhao, K Maddali, SJ Smith, M Métifiot, BC Johnson, et al., *Biorg. Med. Chem. Lett.*, **2012**, 22, 7309-7313.
[26] C Tintori, J Demeulemeester, L Franchi, S Massa, Z Debyser, et al., *Biorg. Med. Chem. Lett.*, **2012**, 22, 3109-3114.
[27] L Hu, S Zhang, X He, Z Luo, X Wang, et al., *Bioorg. Med. Chem.*, **2012**, 20, 177-182.
[28] J Tang, K Maddali, M Metifiot, YY Sham, R Vince, et al., *J. Med. Chem.*, **2011**, 54, 2282-2292.
[29] J Tang, K Maddali, CD Dreis, YY Sham, R Vince, et al., *Biorg. Med. Chem. Lett.*, **2011**, 21, 2400-2402.
[30] JY Nagasawa, J Song, H Chen, H-W Kim, J Blazel, et al., *Biorg. Med. Chem. Lett.*, **2011**, 21, 760-763.
[31] K Ma, P Wang, W Fu, X Wan, L Zhou, et al., *Biorg. Med. Chem. Lett.*, **2011**, 21, 6724-6727.
[32] MA Quevedo, SR Ribone, MC Briñón, W Dehaen, *J. Mol. Graph. Mod.*, **2014**, 52, 82-90.
[33] Z Zhang, B Wang, B Wan, L Yu, Q Huang, *Biochem. Biophys. Res. Comm.*, **2013**, 436, 650-654.

[34] H Sharma, X Cheng, JK Buolamwini, *J. Chem. Inf. Mod.*, **2012**, 52, 515-544.
[35] K Majerz-Maniecka, R Musiol, A Skórska-Stania, D Tabak, P Mazur, et al., *Bioorg. Med. Chem.*, **2011**, 19, 1606-1612.
[36] M Sippel, CA Sotriffer, *J. Chem. Inf. Mod.*, **2010**, 50, 604-614.
[37] P Selvam, M Chandramohan, NS Prabhu, MS Kumar, *Antivir. Res.*, **2010**, 86, A45.
[38] P Lu, X Wei, R Zhang, *Eur. J. Med. Chem.*, **2010**, 45, 3413-3419.
[39] P Vandurm, C Cauvin, J Wouters, EA Perpète, D Jacquemin, *Chem. Phys. Lett.*, **2009**, 478, 243-248.
[40] P Vandurm, C Cauvin, A Guiguen, B Georges, KL Van, et al., *Biorg. Med. Chem. Lett.*, **2009**, 19, 4806-4809.
[41] P Gupta, N Roy, P Garg, *Eur. J. Med. Chem.*, **2009**, 44, 4276-4287.
[42] JT Leonard, K Roy, *Eur. J. Med. Chem.*, **2008**, 43, 81-92.
[43] N Nunthaboot, S Pianwanit, V Parasuk, S Kokpol, P Wolschann, *J. Mol. Struct.*, **2007**, 844–845, 208-214.
[44] N Nunthaboot, S Pianwanit, V Parasuk, JO Ebalunode, JM Briggs, et al., *Biophys. J.*, **2007**, 93, 3613-3626.
[45] M Iyer, AJ Hopfinger, *J. Chem. Inf. Mod.*, **2007**, 47, 1945-1960.
[46] K Majerz-Maniecka, R Musiol, W Nitek, BJ Oleksyn, J-F Mouscadet, et al., *Biorg. Med. Chem. Lett.*, **2006**, 16, 1005-1009.
[47] D Firley, B Courcot, J-M Gillet, B Fraisse, F Zouhiri, et al., *J. Phys. Chem. B*, **2006**, 110, 537-547.
[48] Y Marrero-Ponce, *J. Chem. Info. Comp. Sci.*, **2004**, 44, 2010-2026.
[49] C-L Kuo, H Assefa, S Kamath, Z Brzozowski, J Slawinski, et al., *J. Med. Chem.*, **2004**, 47, 385-399.
[50] ML Barreca, KW Lee, A Chimirri, JM Briggs, *Biophys. J.*, **2003**, 84, 1450-1463.
[51] JK Buolamwini, H Assefa, *J. Med. Chem.*, **2002**, 45, 841-852.
[52] MT Makhija, VM Kulkarni, *J. Chem. Info. Comp. Sci.*, **2001**, 41, 1569-1577.
[53] JS Gómez-Jeria, M Flores-Catalán, *Canad. Chem. Trans.*, **2013**, 1, 215-237.
[54] DA Alarcón, F Gatica-Díaz, JS Gómez-Jeria, *J. Chil. Chem. Soc.*, **2013**, 58, 1651-1659.
[55] F Soto-Morales, JS Gómez-Jeria, *J. Chil. Chem. Soc.*, **2007**, 52, 1214-1219.
[56] BA Johns, T Kawasuji, JG Weatherhead, EE Boros, JB Thompson, et al., *Biorg. Med. Chem. Lett.*, **2014**, 24, 3104-3107.
[57] JS Gómez-Jeria, *Canad. Chem. Trans.*, **2013**, 1, 25-55.
[58] JS Gómez-Jeria, *Elements of Molecular Electronic Pharmacology (in Spanish)*, Ediciones Sokar, Santiago de Chile, **2013**.
[59] T Bruna-Larenas, JS Gómez-Jeria, *Int. J. Med. Chem.*, **2012**, 2012 Article ID 682495, 1-16.
[60] JS Gómez-Jeria, M Ojeda-Vergara, *J. Chil. Chem. Soc.*, **2003**, 48, 119-124.
[61] JS Gómez-Jeria, "Modeling the Drug-Receptor Interaction in Quantum Pharmacology," in *Molecules in Physics, Chemistry, and Biology*, J. Maruani Ed., vol. 4, pp. 215-231, Springer Netherlands, 1989.
[62] JS Gómez-Jeria, *Il Far. (Ed. Sci).* **1985**, 40, 299-302.
[63] JS Gómez-Jeria, *Int. J. Quant. Chem.*, **1983**, 23, 1969-1972.
[64] JM Boeynaems, JE Dumont, *Outlines of receptor theory*, Elsevier/North-Holland Biomedical Press, Amsterdam, **1980**.
[65] JS Gómez-Jeria, J Valdebenito-Gamboa, *Der Pharma Chem.*, **2015**, 7, 323-347.
[66] JS Gómez-Jeria, A Robles-Navarro, *Res. J. Pharmac. Biol. Chem. Sci.*, **2015**, 6, 1358-1373.
[67] JS Gómez-Jeria, A Robles-Navarro, *Res. J. Pharmac. Biol. Chem. Sci.*, **2015**, 6, 1811-1841.
[68] JS Gómez-Jeria, A Robles-Navarro, *J. Comput. Methods Drug Des.*, **2015**, 5, 15-26.
[69] JS Gómez-Jeria, A Robles-Navarro, *Der Pharma Chem.*, **2015**, 7, 243-269.
[70] R Solís-Gutiérrez, JS Gómez-Jeria, *Res. J. Pharmac. Biol. Chem. Sci.*, **2014**, 5, 1401-1416.
[71] F Salgado-Valdés, JS Gómez-Jeria, *J. Quant. Chem.*, **2014**, 2014 Article ID 431432, 1-15.
[72] JS Gómez-Jeria, J Valdebenito-Gamboa, *Der Pharma Chem.*, **2014**, 6, 383-406.
[73] JS Gómez-Jeria, J Molina-Hidalgo, *J. Comput. Methods Drug Des.*, **2014**, 4, 1-9.
[74] JS Gómez-Jeria, *Res. J. Pharmac. Biol. Chem. Sci.*, **2014**, 5, 424-436.
[75] JS Gómez-Jeria, *Res. J. Pharmac. Biol. Chem. Sci.*, **2014**, 5, 2124-2142.
[76] JS Gómez-Jeria, *SOP Trans. Phys. Chem.*, **2014**, 1, 10-28.
[77] JS Gómez-Jeria, *Der Pharm. Lett.*, **2014**, 6., 95-104.
[78] JS Gómez-Jeria, *J. Chil. Chem. Soc.*, **2010**, 55, 381-384.
[79] JS Gómez-Jeria, F Soto-Morales, J Rivas, A Sotomayor, *J. Chil. Chem. Soc.*, **2008**, 53, 1393-1399.
[80] JS Gómez-Jeria, LA Gerli-Candia, SM Hurtado, *J. Chil. Chem. Soc.*, **2004**, 49, 307-312.
[81] JS Gómez-Jeria, F Soto-Morales, G Larenas-Gutierrez, *Ir. Int. J. Sci.*, **2003**, 4, 151-164.
[82] JS Gómez-Jeria, L Lagos-Arancibia, E Sobarzo-Sánchez, *Bol. Soc. Chil. Quím.*, **2003**, 48, 61-66.
[83] JS Gómez-Jeria, L Lagos-Arancibia, *Int. J. Quant. Chem.*, **1999**, 71, 505-511.

[84] JS Gómez-Jeria, M Ojeda-Vergara, *Int. J. Quant. Chem.*, **1997**, 61, 997-1002.
[85] JS Gómez-Jeria, M Ojeda-Vergara, C Donoso-Espinoza, *Mol. Engn.*, **1995**, 5, 391-401.
[86] JS Gómez-Jeria, P Sotomayor, *J. Mol. Struct. (Theochem)*, **1988**, 166, 493-498.
[87] JS Gómez-Jeria, D Morales-Lagos, BK Cassels, JC Saavedra-Aguilar, *Quant. Struct.-Relat.*, **1986**, 5, 153-157.
[88] JS Gómez-Jeria, D Morales-Lagos, JI Rodriguez-Gatica, JC Saavedra-Aguilar, *Int. J. Quant. Chem.*, **1985**, 28, 421-428.
[89] JS Gómez-Jeria, DR Morales-Lagos, *J. Pharm. Sci.*, **1984**, 73, 1725-1728.
[90] JS Gómez-Jeria, D Morales-Lagos, "The mode of binding of phenylalkylamines to the Serotonergic Receptor," in *QSAR in design of Bioactive Drugs*, M. Kuchar Ed., pp. 145-173, Prous, J.R., Barcelona, Spain, **1984**.
[91] JS Gómez-Jeria, J Valdebenito-Gamboa, *Der Pharm. Lett.*, **2015**, 7, 211-219.
[92] JS Gómez-Jeria, A Robles-Navarro, *Res. J. Pharmac. Biol. Chem. Sci.*, **2015**, 6, 755-783.
[93] JS Gómez-Jeria, A Robles-Navarro, *Res. J. Pharmac. Biol. Chem. Sci.*, **2015**, 6, 1337-1351.
[94] JS Gómez-Jeria, *Res. J. Pharmac. Biol. Chem. Sci.*, **2015**, 6, 688-697.
[95] DI Pino-Ramírez, JS Gómez-Jeria, *Amer. Chem. Sci. J.*, **2014**, 4, 554-575.
[96] D Muñoz-Gacitúa, JS Gómez-Jeria, *J. Comput. Methods Drug Des.*, **2014**, 4, 48-63.
[97] D Muñoz-Gacitúa, JS Gómez-Jeria, *J. Comput. Methods Drug Des.*, **2014**, 4, 33-47.
[98] JS Gómez-Jeria, *Res. J. Pharmac. Biol. Chem. Sci.*, **2014**, 5, 780-792.
[99] JS Gómez-Jeria, *J. Comput. Methods Drug Des.*, **2014**, 4, 38-47.
[100] JS Gómez-Jeria, *J. Comput. Methods Drug Des.*, **2014**, 4, 32-44.
[101] JS Gómez-Jeria, *Der Pharma Chem.*, **2014**, 6, 64-77.
[102] JS Gómez-Jeria, *Brit. Microbiol. Res. J.*, **2014**, 4, 968-987.
[103] JS Gómez-Jeria, *Int. Res. J. Pure App. Chem.*, **2014**, 4, 270-291.
[104] F Gatica-Díaz, JS Gómez-Jeria, *J. Comput. Methods Drug Des.*, **2014**, 4, 79-120.
[105] I Reyes-Díaz, JS Gómez-Jeria, *J. Comput. Methods Drug Des.*, **2013**, 3, 11-21.
[106] A Paz de la Vega, DA Alarcón, JS Gómez-Jeria, *J. Chil. Chem. Soc.*, **2013**, 58, 1842-1851.
[107] C Barahona-Urbina, S Nuñez-Gonzalez, JS Gómez-Jeria, *J. Chil. Chem. Soc.*, **2012**, 57, 1497-1503.
[108] MJ Frisch, GW Trucks, HB Schlegel, GE Scuseria, MA Robb, et al., "G03 Rev. E.01," Gaussian, Pittsburgh, PA, USA, **2007**.
[109] JS Gómez-Jeria, *J. Chil. Chem. Soc.*, **2009**, 54, 482-485.
[110] RS Mulliken, *J. Chem. Phys.*, **1955**, 23, 1833-1840.
[111] JS Gómez-Jeria, "D-Cent-QSAR: A program to generate Local Atomic Reactivity Indices from Gaussian 03 log files. 1.0," Santiago, Chile, **2014**.
[112] Statsoft, "Statistica 8.0," 2300 East 14 th St. Tulsa, OK 74104, USA, 1984-**2007**.
[113] LB Kier, *Molecular orbital studies in chemical pharmacology*, Springer, Berlin, Heidelberg, New York, **1970**.
[114] JA Pople, DL Beveridge, *Approximate molecular orbital theory*, McGraw-Hill, New York, **1970**.
[115] LB Kier, *Molecular orbital theory in drug research*, Academic Press, New York, **1971**.
[116] LB Kier, LH Hall, *Molecular connectivity in chemistry and drug research*, Academic Press, New York, **1976**.
[117] GA Segal, *Semiempirical methods of electronic structure calculation*, Plenum Press, New York, **1977**.